JPPIPA 12(5) (2026)

Jurnal Penelitian Pendidikan IPA

http://jppipa.unram.ac.id/index.php/jppipa/index

Modeling Aboveground Biomass and Stand Density Using Forest Canopy Density in a Tropical Natural Forest Concession

Reza Dwiputra Perdhana[1*], Lilik Budi Prasetyo[1], Rachmad Hermawan[1]

[1] Tropical Biodiversity Conservation Study Program, Graduate School, IPB University, Bogor, Indonesia.

Received: March 11, 2026
Revised: April 06, 2026
Accepted: May 25, 2026
Published: May 31, 2026

Corresponding Author:
Reza Dwiputra Perdhana
rezadforester@gmail.com

DOI: 10.29303/jppipa.v12i5.14793

Abstract: Natural forests within the concession area of PT Bharinto Ekatama are critical for carbon storage and ecosystem service provision, yet efficient methods to quantify stand biophysical parameters at scale remain limited. This study developed spatial models to estimate stand density and aboveground biomass using the Forest Canopy Density (FCD) approach. Field data were collected from 30 plots (50 × 50 m) between January and June 2025, complemented by Landsat 8 OLI/TIRS imagery. FCD was derived from the integration of Advanced Vegetation, Bare Soil, Shadow, and Thermal indices. Relationships between FCD and field-based measurements were evaluated using linear regression. The forest community comprised 47 species across 21 families, dominated by Dipterocarpus. FCD values ranged from 49.05% to 85.22%, while aboveground biomass and stand density ranged from 37.36–331.65 ton ha^{-1} and 660–2,224 trees ha^{-1}, respectively. The models demonstrated strong explanatory power (R^2 = 0.8335 for stand density; R^2 = 0.8317 for biomass; $p < 0.05$). Validation yielded RMSE values of 151.662 trees ha^{-1} and 29.695 ton ha^{-1}, corresponding to normalized errors of 12% and 22%. These findings indicate that the FCD approach provides a robust and scalable framework for estimating forest structure, with greater predictive accuracy for stand density than biomass.

Keywords: Aboveground biomass; Forest canopy density; Stand density

Introduction

Global climate change has positioned carbon-related environmental services as a central issue in natural resource management. Tropical forests function as major carbon sinks, storing substantial carbon in aboveground biomass and regulating the global climate system (Dasrizal et al., 2019). From a forest ecology perspective, stand structure—particularly stand density and canopy cover—plays a key role in determining biomass accumulation and carbon storage capacity (Chave et al., 2014). Changes in canopy structure directly influence microclimatic conditions, regeneration processes, and overall ecosystem functioning. Consequently, disturbances such as open-pit coal mining not only remove vegetation but also disrupt forest structure and carbon dynamics, leading to significant CO_2 emissions (Xu et al., 2024).

In Indonesia, particularly in East Kalimantan, mining-driven land cover change has resulted in substantial forest loss and carbon emissions. Kartikasari et al. (2019) reported 12,663.28 ha of land conversion associated with mining activities, contributing to 0.60 Mton CO_2-eq emissions. Similarly, Dwiyanto et al. (2021) identified a continuous decline in forest area alongside mining expansion based on Landsat analysis from 2009 to 2019. Reductions in canopy density are associated with declining biodiversity, altered microclimates, and reduced ecosystem resilience (Judijanto & Adiwijaya, 2024), highlighting the importance of monitoring forest structural attributes as key indicators of ecosystem condition.

Within mining concessions, some forest fragments are retained because they carry biodiversity and ecosystem-service value, and recent conservation planning studies show that mining concessions can still drive substantial forest loss and fragmentation.

How to Cite:
Perdhana, R. D., Prasetyo, L. B., & Hermawan, R. (2026). Modeling Aboveground Biomass and Stand Density Using Forest Canopy Density in a Tropical Natural Forest Concession . *Jurnal Penelitian Pendidikan IPA*, *12*(5), 762–774. https://doi.org/10.29303/jppipa.v12i5.14793

Fragments of natural forest are often retained based on ecological and regulatory considerations, including biodiversity value, hydrological function, slope stability, and conservation priorities (Fiqa et al., 2018; Siqueira-Gay et al., 2020; Williams et al., 2022). These remnant forests play a strategic role as carbon reservoirs and reference ecosystems for evaluating ecological recovery. Studies in East Kalimantan show that natural forests surrounding mining areas can store significant carbon stocks, ranging from 161.93 ton/ha (Fiqa et al., 2025) to 296.8-ton C/ha (Fauziah et al., 2021). In addition, proximity to natural forests enhances regeneration processes in degraded areas (Morales-Parra et al., 2020).

At the same time, reclamation and revegetation efforts are implemented to restore ecosystem functions in post-mining landscapes. Reforestation has been recognized as an important strategy for climate change mitigation (Asum et al., 2025). Empirical studies show that revegetation can recover up to 70% of baseline carbon stocks within a decade (Farosandi et al., 2024), with continued increases over time (Arifin, 2025). However, carbon recovery trajectories are often non-linear, as some reclamation areas exhibit low carbon stocks despite increasing age (Fiqa et al., 2025), emphasizing the need for systematic and spatial monitoring.

Conventional field-based inventories provide accurate estimates of stand density and biomass but are constrained by time, cost, and accessibility limitations. Remote sensing offers an efficient alternative for large-scale monitoring. The Forest Canopy Density (FCD) model integrates spectral indices Advanced Vegetation Index (AVI), Bare Soil Index (BSI), Shadow Index (SI), and Thermal Index (TI) to estimate canopy density and its relationship with forest structure (Rikimaru et al., 2002). Previous studies have demonstrated the applicability of FCD in estimating forest biophysical parameters, with varying levels of correlation (Hartoyo et al., 2019; Sukarna et al., 2021). Aguswan et al. (2022) further reported strong relationships between FCD values and stand structural attributes (R = 0.87–0.97).

Despite its application, several research gaps remain. Existing studies generally focus on single variables, such as canopy density, stand density, or carbon stock, without developing integrated models. In addition, FCD applications are predominantly conducted in protected forests or reclamation areas, with limited focus on natural forest fragments within active mining concessions (Rosikin et al., 2023). Furthermore, most studies are descriptive and lack predictive modeling frameworks suitable for periodic monitoring.

Therefore, this study aims to develop spatial models for estimating stand density and aboveground biomass using the FCD approach in natural forests within the concession area of PT Bharinto Ekatama. This study provides a site-specific and scalable framework for monitoring forest structure and carbon-related ecosystem services in mining landscapes.

Method

The study was conducted within the concession area of PT Bharinto Ekatama, located in Damai and Teweh Timur sub-districts. Field data collection was carried out from June to November 2025. Primary data were obtained through field measurements in 30 sample plots, each measuring 50 × 50 m. Within each plot, diameter at breast height (DBH) was recorded and classified into three growth stages: saplings (DBH < 10 cm), poles (DBH 10–20 cm), and trees (DBH > 20 cm). Additional parameters recorded included the number of individuals, species composition, and plot coordinates. These data were subsequently used to calculate stand density and aboveground biomass. The study area map is presented in Figure 1.

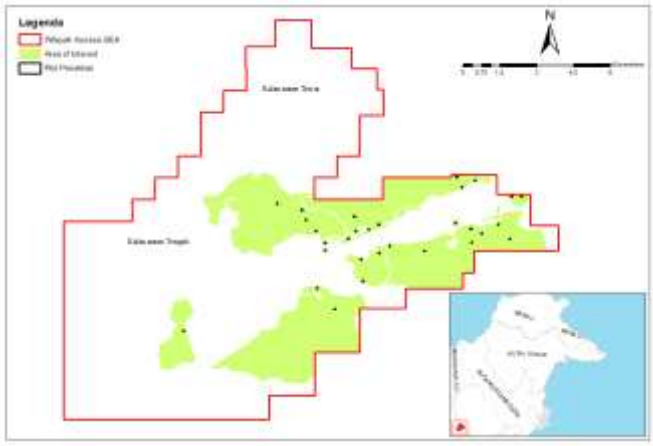

Figure 1. Study area of PT Bharinto Ekatama concession

The analytical procedure commenced with the processing of Landsat 8 imagery to derive Forest Canopy Density (FCD) values. Image preprocessing involved atmospheric correction, cloud masking, and the computation of the spectral indices constituting the FCD model, namely the Advanced Vegetation Index (AVI), Bare Soil Index (BI), Shadow Index (SI), and Thermal Index (TI). These indices were then transformed using Principal Component Analysis (Komara et al., 2023; Rosikin et al., 2023).

Subsequently, the transformed indices were integrated to generate spatially explicit FCD values representing variations in canopy density across the study area. Field-based measurements, including stand density and tree diameter, were collected from vegetation plots and used to estimate aboveground biomass through established allometric equations. The relationship between FCD values and field-derived

parameters was then analyzed using linear regression to develop predictive models. Model performance was evaluated using the coefficient of determination (R^2) and Root Mean Square Error (RMSE), followed by normalization (NRMSE) to assess model accuracy.

The overall workflow of the research, encompassing image processing, field data collection, model development, and validation, is illustrated in the following figure 2.

Figure 2. Research workflow

As illustrated in Figure 2, the analytical workflow integrates image processing and field data analysis to derive FCD-based models. Following this framework, the spectral indices comprising the FCD model were calculated using the following formula:

Advanced Vegetation Index (AVI)

$$\sqrt[3]{(\text{Band 5} + 1) \times (65536 - \text{Band 4}) \times (\text{Band 5} - \text{Band 4})} \quad (1)$$

Bare Soil Index (BI)

$$((\text{Band 6} + \text{Band 4}) - (\text{Band 5} + \text{Band 2})) / ((\text{Band 6} + \text{Band 4}) + (\text{Band 5} + \text{Band 2})) \times 100 + 100 \quad (2)$$

Shadow Index (SI)

$$\sqrt[3]{(256 - \text{Band 2}) \times (256 - \text{Band 3}) \times (256 - \text{Band 4})} \quad (3)$$

Thermal Indeks (TI)

$$TI = K2 / Ln(K1/L\ \lambda + 1) \quad (4)$$

Principal Component Analysis (PCA) was performed using the Principal Components tool in ArcGIS 10.8. Once Vegetation Density (VD) and Scaled Shadow Index (SSI) were obtained, normalization was applied using the equations proposed by Danoedoro et al. (2022) and Falensky et al. (2020).

$$\text{Normalisasi} = (B1 - \min) \times (\max' - \min') / \max - \min \quad (5)$$

Forest Canopy Density (FCD) was subsequently calculated by integrating VD and SSI into a single percentage scale representing canopy cover density, following the equation described by Sediyo et al., (2024).

$$FCD = (SVD \times SSI + 1)1/2 - 1 \quad (6)$$

Aboveground biomass for each plot within the natural forest sites was estimated using the following allometric equation shown in Table 1.

Table 1. Allometric Equations for Different Vegetation Types

Species	Allometric Equation	R^2	Source
Meranti Merah (*Shorea leprosula*)	Y = 0.067*D^2.859	0.98	Manuri et al. (2016); Huy (2016)
Meranti Kuning (*Shorea acuminata*)	ln(TAGB)=−2.193+2.371ln(DBH)	0.98	Huy (2016)
Meranti Putih (*Shorea bracteolata*)	ln(TAGB)=−2.193+2.371ln(DBH)	0.98	Huy (2016)
Medang (*Litsea firma*)	ln(TAGB)=−1,201+2,196ln(DBH)	0.91	Karyati et al. (2023)
Mahang (*Macaranga gigantea*)	ln(TAGB)=−1,201+2,196ln(DBH)	0.91	Karyati et al. (2023)
Jabon (*Anthocephalus cadamba*)	Y = 0.035*D^2,600	0.95	Werdana et al. (2024)
Jambu (*Syzygium polyanthum*)	ln(TAGB)=−1,201+2,196ln(DBH)	0.91	Karyati et al. (2023)
Pulai (*Alstonia scholaris*)	ln(TAGB)=−1,201+2,196ln(DBH)	0.91	Karyati et al. (2023)
Keruing (*Dipterocarpus gracilis*)	ln(TAGB)=−1.232+2.178ln(DBH)	0.96	Manuri et al. (2016); Huy (2016)
Nyatoh (*Palaquium gutta*)	ln(TAGB)=−1.098+2.142ln(DBH)	0.91	Karyati et al. (2023)
Sengon (*Paraserianthes falcataria*)	Y=0.148D^2.39	0.95	Hossain et al. (2023); Werdana et al. (2024)
Jenis pohon lainnya	ln(TAGB)=-1,201+2,196ln(DBH)	-	Karyati et al. (2023)

To characterize the stand structure and species composition within each sample plot, a vegetation analysis was conducted encompassing the following aspects:

KT = (Number of Individuals of a Species)/(Sampling Plot Area) (7)

Statistical analyses were performed, including a normality test, a heteroscedasticity test, and regression analysis. In this study, simple linear regression analysis was employed to examine the relationship between one variable and another, using the following equation (Pandey et al., 2021).

$$\hat{y}=a + bX \quad (8)$$

Model validation was subsequently conducted to assess the accuracy of the predictive model using the following equation (Burt et al., 2020).

$$SA = \frac{\Sigma_{i=1}^{n} \hat{y}_i - \Sigma_{i=1}^{n} y_i}{\Sigma_{i=1}^{n} \hat{y}_i} \quad (9)$$

$$SR = \frac{\Sigma_{i=1}^{n} \frac{(\hat{y}_i - yi)^2}{\hat{y}_i}}{n}$$

$$RMSE = \sqrt{\frac{\Sigma \frac{(y_i - \hat{y}_i)^2}{y_i}}{n}} \times 100\%$$

$$e = \frac{\Sigma_{i=1}^{n} \hat{y}_i - \Sigma_{i=1}^{n} y_i}{n}$$

Results and Discussion

Vegetation Composition

The vegetation analysis identified 43 species belonging to 21 families, indicating relatively high species richness within the study area. The family Dipterocarpaceae was the most dominant, comprising 11 species, followed by Fabaceae with five species. The dominance of Dipterocarpaceae observed in this study is consistent with findings reported in tropical lowland forests of Kalimantan, where dipterocarp species form the upper canopy layer and contribute substantially to forest biomass and carbon storage. This dominance reflects the important ecological role of Dipterocarpaceae in maintaining stand structure and regulating ecosystem stability within tropical natural forests.

The presence of Fabaceae species also indicates the contribution of pioneer and secondary vegetation groups, particularly through nitrogen fixation processes that improve soil fertility and support forest regeneration (Batterman et al., 2018). Similar vegetation dynamics have been reported by Susanto et al. (2016), who found that canopy openings in disturbed tropical forests promote the establishment of light-demanding pioneer species such as Macaranga spp. and Syzygium spp. In this study, the coexistence of pioneer species and late-successional species such as Shorea laevis and Eusideroxylon zwageri suggests that the forest is undergoing an active successional recovery process while still retaining characteristics of mature forest stands. The distribution of vegetation families in the study area is presented in Figure 3.

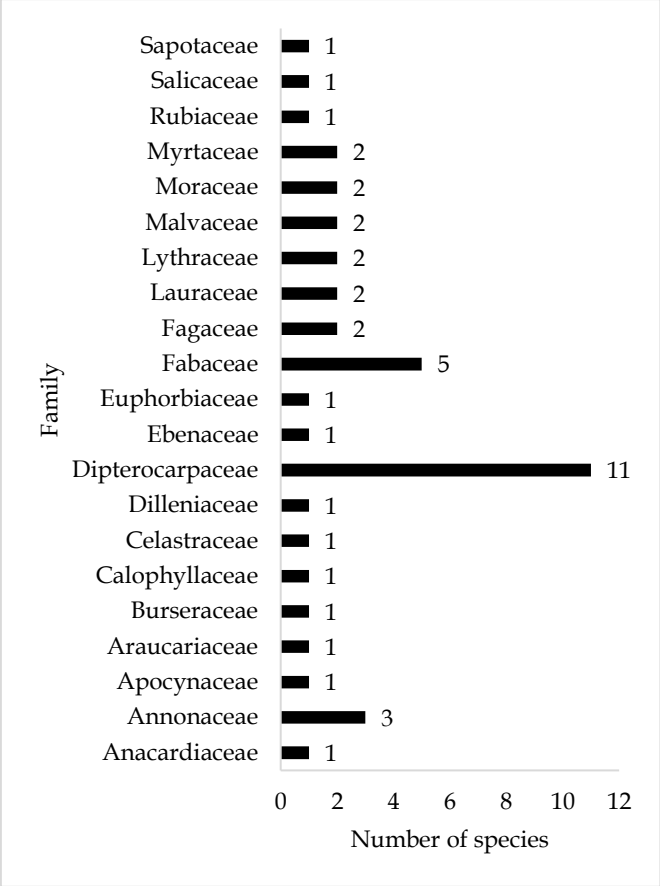

Figure 3. Vegetation distribution by family in the natural forest of PT BEK

The relatively balanced distribution among dominant and non-dominant species further indicates a heterogeneous forest structure with relatively stable ecological interactions. Such species evenness is commonly associated with greater ecosystem resilience and adaptive capacity against environmental disturbances. Similar patterns were also observed by Marjenah et al. (2023), who reported that heterogeneous stand composition in tropical forests contributes positively to regeneration continuity and long-term ecosystem stability. In addition, the Dipterocarpaceae group plays a major role in shaping canopy structure, which directly influences canopy density and contributes to higher biomass estimates observed in this study.

The relatively high proportion of non-dominant species also highlights substantial species richness within the community. These species play important roles in filling ecological niches, maintaining nutrient

cycling, and supporting overall ecosystem functioning. The presence of intermediate species groups, including Macaranga gigantea, Syzygium spp., and Litsea spp., further indicates active regeneration processes, particularly within canopy gaps.

Vegetation Structure

Based on growth stages, 43 species were recorded at the sapling level, 39 at the pole level, and 31 at the tree level. The decreasing trend from sapling to tree stage reflects a typical inverted J-shaped stand structure commonly found in tropical natural forests. Similar patterns were reported by Sukarna et al. (2022) and Marjenah et al. (2023), who explained that continuous regeneration and progressive competition among individuals lead to reduced density at larger growth stages. This condition indicates that natural regeneration within the study area is still actively occurring and that the forest maintains relatively stable structural dynamics.

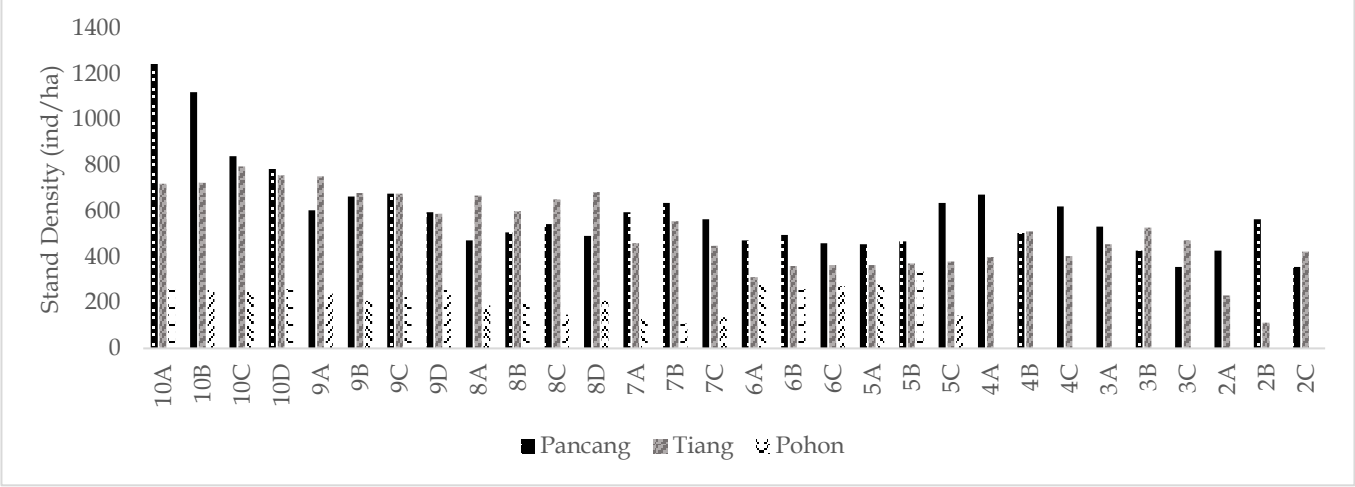

Figure 4. Stand density distribution across growth stages

As shown in Figure 4, saplings consistently exhibited the highest stand density compared to poles and trees. This pattern demonstrates strong regeneration potential, particularly in areas experiencing canopy openings and increased light availability. Comparable findings were reported by Susanto et al. (2016), who observed that disturbed tropical forests often contain high sapling densities due to the rapid establishment of pioneer species following canopy disturbance.

Variations in stand density among plots also indicate differences in disturbance history, stand age, and site conditions. Plots dominated by pioneer species generally exhibited lower canopy closure and lower FCD values, while plots containing mature dipterocarp species showed denser canopy structures and higher biomass accumulation. This finding supports the study of Hartoyo et al. (2019), which demonstrated that canopy cover exerts a stronger influence on FCD values than tree density alone. Therefore, the observed heterogeneity in stand structure reflects the combined influence of regeneration processes, environmental conditions, and canopy complexity within mining-associated tropical forest landscapes.

In Class 2, the stand is dominated by saplings with limited canopy closure, likely due to young vegetation age and suboptimal soil conditions, including low pH and nutrient availability (Agus et al., 2014). In addition, enrichment planting contributes to structural heterogeneity and canopy gaps. These conditions influence FCD values, as the model is sensitive to canopy cover and openings (Chandrashekhar et al., 2005; Wang et al., 2022). Consequently, the relatively low FCD value in Class 2 (49.05%) reflects the combined effects of young stands, edaphic limitations, and canopy heterogeneity.

Forest Canopy Density Index

The integration of AVI, BSI, SI, and TI within the Forest Canopy Density (FCD) model provides significant advantages compared to single vegetation indices such as NDVI. Unlike NDVI, which primarily reflects vegetation greenness, the FCD model incorporates thermal characteristics, shadow intensity, and bare soil exposure, enabling a more comprehensive representation of forest structure (Rikimaru et al., 2002). Similar conclusions were reported by Ashaari et al. (2018), Atmojo et al. (2024) and Tian et al. (2023), who demonstrated that multi-index approaches generally produce higher accuracy in estimating canopy density and forest structural conditions.

In this study, AVI values range from 55.49 to 121.64, indicating vegetation conditions from moderate to relatively dense canopy cover. AVI values increased proportionally with canopy density and biomass, indicating that near-infrared reflectance effectively

captured variations in vegetation cover. Comparable results have been reported by recent remote-sensing studies, where satellite-based canopy-density methods and near-infrared vegetation metrics were shown to capture tropical forest canopy structure and heterogeneity effectively (Abdollahnejad et al., 2017; Merrick et al., 2021; Ashaari et al., 2018) who reported strong relationships between NIR-based indices and tropical forest canopy characteristics. However, spectral saturation remains a limitation in dense tropical forests, particularly in areas with highly closed canopies (Mutanga et al., 2023; Zhao et al., 2016). The processed FCD index results are presented in Figure 5.

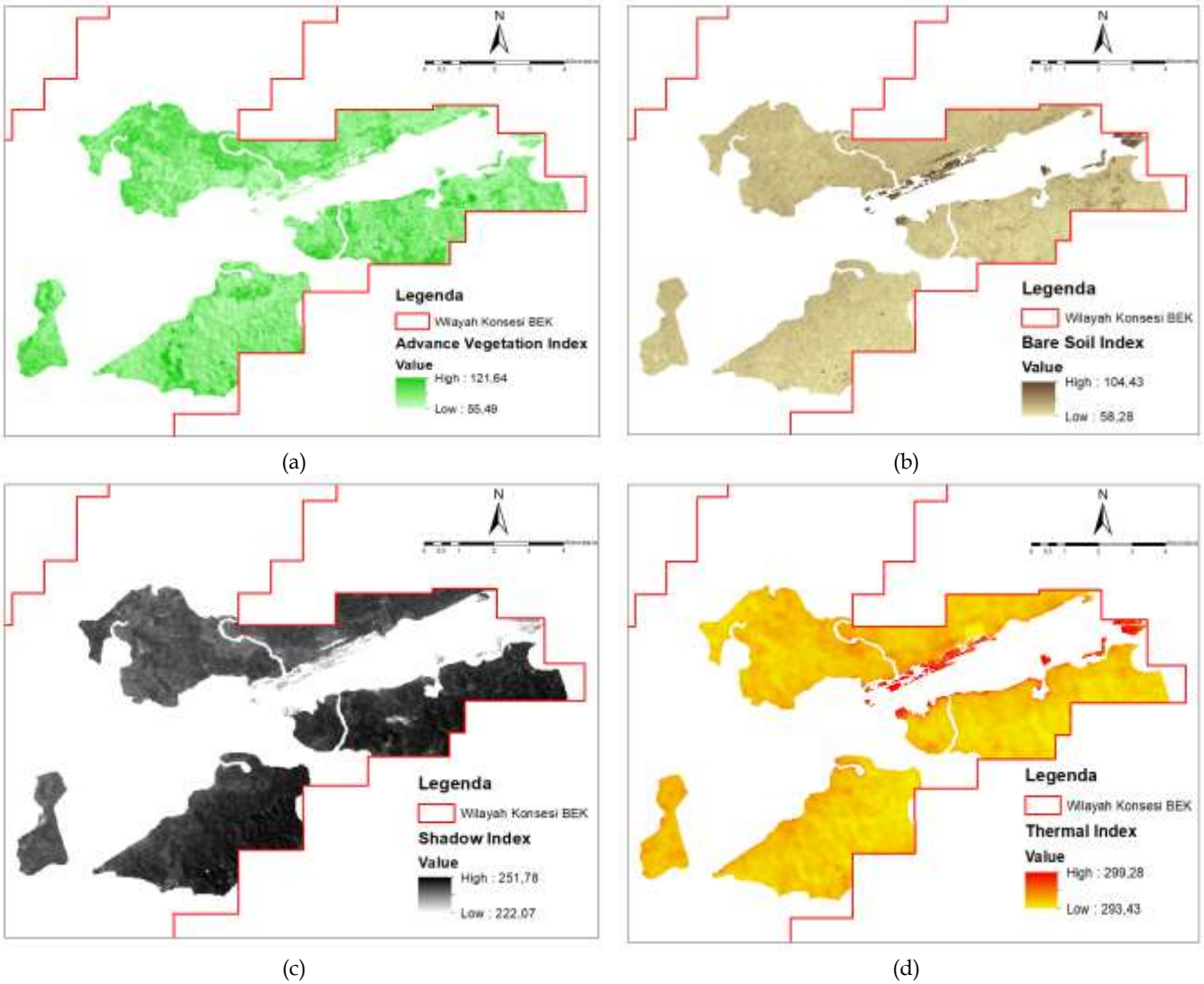

Figure 5 Results of the Forest Canopy Density (FCD) index processing: (a) Advanced Vegetation Index (AVI); (b) Bare Soil Index (BSI); (c) Shadow Index (SI); (d) Thermal Index (TI)

Higher AVI values correspond to areas with well-developed canopy structures and strong near-infrared (NIR) reflectance, which is closely associated with higher biomass and vegetation density (Roy et al., 1997; Rikimaru et al., 2002). Conversely, lower AVI values represent areas with reduced canopy density. This variation reflects the heterogeneity of tropical forest canopy structure (Chandrashekhar et al., 2005). The sensitivity of NIR-based indices to vegetation structure has been widely reported, although it tends to saturate at high canopy densities (Gao et al., 2023). The integration of AVI within the FCD framework has been shown to effectively estimate vegetation density, with comparable or higher accuracy than alternative indices (Ashaari et al., 2018; Fahmi et al., 2025).

In contrast, BSI values range from 58.28 to 104.43, indicating variability in the proportion of exposed soil and vegetation cover. Higher BSI values represent areas dominated by bare soil or sparse vegetation, characterized by higher reflectance in red and SWIR bands. Lower BSI values indicate denser vegetation with stronger NIR reflectance. Within the FCD model, BSI

functions as an inverse indicator of vegetation density, complementing AVI in distinguishing vegetated and non-vegetated surfaces (Rikimaru et al., 2002). This relationship has been confirmed in recent studies showing that higher BSI values correspond to lower vegetation cover (Andini et al., 2024).

The SI values, ranging from 222.07 to 251.78, represent variation in canopy shadow intensity, which is closely related to vertical forest structure. Higher SI values indicate dense vegetation with complex canopy stratification and higher biomass, while lower values correspond to more open canopy conditions. Unlike spectral vegetation indices, SI provides additional information on vertical canopy complexity, which is essential for accurately representing forest structure within the FCD model (Rikimaru et al., 2002).

Meanwhile, TI values range from 293.43 K (20.28°C) to 299.28 K (26.13°C), reflecting variations in land surface temperature associated with canopy cover. Higher temperatures are observed in open areas, while lower temperatures are associated with dense vegetation due to the cooling effect of evapotranspiration. This inverse relationship between surface temperature and vegetation density has been widely documented (Mildrexler et al., 2011). Within the FCD framework, TI enhances the differentiation between vegetated and non-vegetated surfaces based on thermal characteristics (Debnath & Mukherjee, 2020).

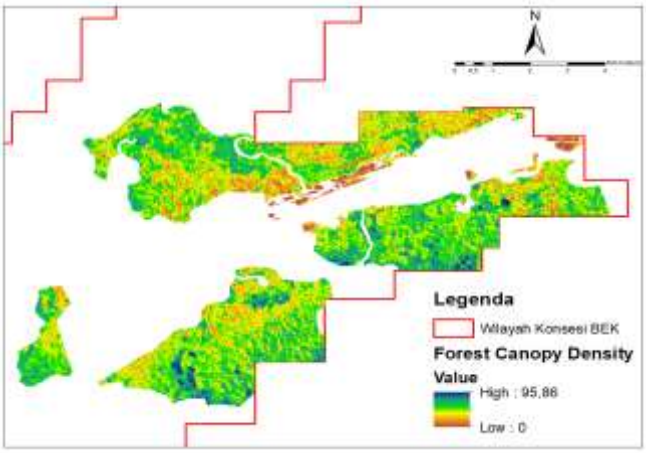

Figure 6. FCD processing results

Overall, the integration of AVI, BSI, SI, and TI within the FCD model effectively captures both horizontal and vertical variations in canopy structure. The observed variability across indices reflects the heterogeneous condition of the forest, influenced by differences in canopy density, vegetation structure, and disturbance history. This multi-index approach provides a robust basis for estimating forest canopy density, which is closely linked to stand density and aboveground biomass in tropical forest ecosystems. The spatial distribution of FCD across the study area is illustrated in Figure 6.

FCD was derived from Landsat 8 OLI/TIRS imagery (2025) using integrated spectral indices—AVI, BSI, SI, and TI—to represent canopy density and land cover characteristics. The resulting FCD values ranged from 0 to 91.86%, indicating substantial spatial variability in vegetation density across the study area. As illustrated in Figure 6, higher FCD values are concentrated in natural forest areas, while lower values are associated with reclamation and open land. This spatial pattern aligns with the conceptual basis of the FCD model, where canopy density increases with vegetation cover and structural complexity (Rikimaru et al., 2002), and is consistent with findings from Andini et al. (2024).

Table 2. The Values of Aboveground Biomass, Stand Density, and FCD for Each Plot

Plot	Biomass (ton/ha)	Stand Density (ind/ha)	FCD Value (%)
10A	264.28	2100	84.37
10B	331.65	2224	85.22
10C	254.34	1892	84.10
10D	250.15	1800	84.31
9A	220.34	1596	81.07
9B	220.20	1552	79.90
9C	190.25	1580	81.01
9D	195.14	1440	80.31
8A	136.21	1328	76.44
8B	141.28	1308	75.48
8C	151.29	1344	76.49
8D	155.19	1384	76.82
7A	132.06	1196	73.49
7B	135.01	1300	74.07
7C	122.29	1148	72.75
6A	112.43	1064	70.49
6B	114.41	1116	70.31
6C	119.41	1096	69.67
5A	95.35	1100	67.24
5B	109.13	1176	67.44
5C	102.03	1160	67.52
4A	89.14	1072	64.98
4B	82.07	1016	62.97
4C	84.39	1024	64.42
3A	69.02	988	58.64
3B	65.16	956	58.53
3C	59.45	828	57.00
2A	37.36	660	49.05
2B	40.18	676	49.72
2C	51.33	780	50.53

Field data (Table 2) show a clear positive relationship between FCD, stand density, and aboveground biomass. The values of aboveground biomass, stand density, and FCD for each plot are presented in Table 2.

The lower FCD values in reclamation areas reflect younger stand age, simpler canopy structure, and more uniform planting patterns dominated by fast-growing species such as Anthocephalus cadamba and Falcataria moluccana. While these species facilitate early-stage recovery, their structural contribution remains limited compared to natural forests. This distinction is consistent with previous studies showing that reclamation areas require extended time to develop structural complexity comparable to secondary forests (Yuningsih et al., 2021; Yunanto et al., 2019), with gradual improvements in diversity and biomass over time (Isworo et al., 2025).

Overall, the observed FCD variation captures the gradient of vegetation condition from early-stage reclamation to more structurally complex natural forests, demonstrating its utility as a reliable proxy for assessing stand density and biomass in mining landscapes.

Statistical Model Testing

Prior to regression modeling, classical assumption tests were conducted to ensure the validity of the statistical analysis. The Shapiro–Wilk test indicated that both stand density ($p = 0.113$) and biomass ($p = 0.054$) followed a normal distribution ($p > 0.05$), satisfying a key requirement for parametric methods. Although the biomass variable showed a value close to the threshold, such minor deviations are generally acceptable in remote sensing-based modelling and do not substantially affect parameter estimation. The Glejser test further confirmed the absence of heteroscedasticity ($p > 0.05$), indicating homoscedastic residuals and reliable variance estimates for both models. The significance values (p-values) of the normality and heteroscedasticity tests for the study variables are presented in Table 3.

Table 3. Normality and Heteroscedasticity Test Results

Variable	Significance	
	Normalities	Heteroskedasticities
Biomass	0.054	0.174
Stand Density	0.113	0.073

Model validation results demonstrate good predictive performance of the FCD-based models. Aggregate deviation and bias values are close to zero, indicating minimal systematic error and no tendency toward over- or underestimation. The normalized RMSE (NRMSE) values of 12% for stand density and 22% for biomass fall within acceptable accuracy ranges for forest parameter estimation, with stand density showing higher precision. This difference reflects the more direct relationship between canopy spectral characteristics and stands density, whereas biomass is influenced by additional structural variables, such as tree diameter and vertical complexity, which are not fully captured by spectral indices. Overall, these results confirm that the developed models are statistically robust and reliable, particularly for estimating stand density in heterogeneous tropical forest landscapes.

Model validation results indicate good performance for both variables. The aggregate deviation (SA) values are close to zero for both stand density (0.00076) and biomass (0.00005), indicating the absence of systematic aggregate bias (Saleh et al., 2024). The bias values are also very small less than one individual per hectare for stand density (0.962) and near zero for biomass (-0.00017) suggesting that the models do not exhibit tendencies toward overestimation or underestimation. The validation results of the Forest Canopy Density (FCD) model in predicting stand density and biomass are presented in Table 4.

Table 4. Statistical Relationship between FCD and Biomass and Stand Density

Parameter	FCD–Stand Density Relationship	FCD–Biomass Relationship
Aggregate deviation (SA)	0.000761	0.000051
Mean deviation (SR)	0.000025	0.000002
Bias (e)	0.96208	-0.00017
RMSE	151.662	29.695
NRMSE (%)	12%	22%

Persson et al. (2020) emphasized that in forest remote sensing studies, bias values approaching zero represent a key indicator of model reliability in estimating forest parameters. The NRMSE value of 12% for stand density is considered good, based on Zhang et al. (2022), who stated that error levels below 20% are comparable to or better than conventional inventory methods. For biomass, the NRMSE value of 22% remains substantially lower than the range of 37–67% reported by Rodríguez-Veiga et al. (2019) in cross-biome biomass estimation studies.

The difference in NRMSE values between the two variables indicates that FCD performs better in representing stand density, as this parameter has a more direct relationship with canopy spectral characteristics (Hartoyo et al., 2019). In contrast, biomass is influenced by additional factors such as tree diameter and vegetation structure, which are not fully captured by spectral indices.

The validation results demonstrate that both models exhibit good performance. Aggregate deviation (SA) values are close to zero for both stand density (0.00076) and biomass (0.00005), indicating the absence of systematic aggregate errors (Saleh et al., 2024). The bias value for biomass, which is also close to zero, further confirms that the model does not exhibit

tendencies toward overestimation or underestimation (Persson and Stahl, 2020). Overall, these results highlight the robustness of the FCD-based models, particularly in estimating stand density compared to biomass.

The regression plots in Figure 7 show a positive correlation between FCD index values and both stand density and biomass. This positive relationship indicates that increases in FCD values are followed by increases in stand density and biomass. The R^2 values in both models can be explained by several factors.

In this study, the use of 10 FCD classes provides finer gradation than previous studies (e.g., Hartoyo et al., 2019), improving the sensitivity of regression modelling. Nevertheless, limitations remain due to spectral saturation in dense canopies and the inability of optical data to fully capture vertical complexity, indicating that FCD is more suitable as a proxy for canopy structure rather than an exact estimator of absolute biomass (Asner, 2009; Lu et al., 2006; Foody et al., 2003).

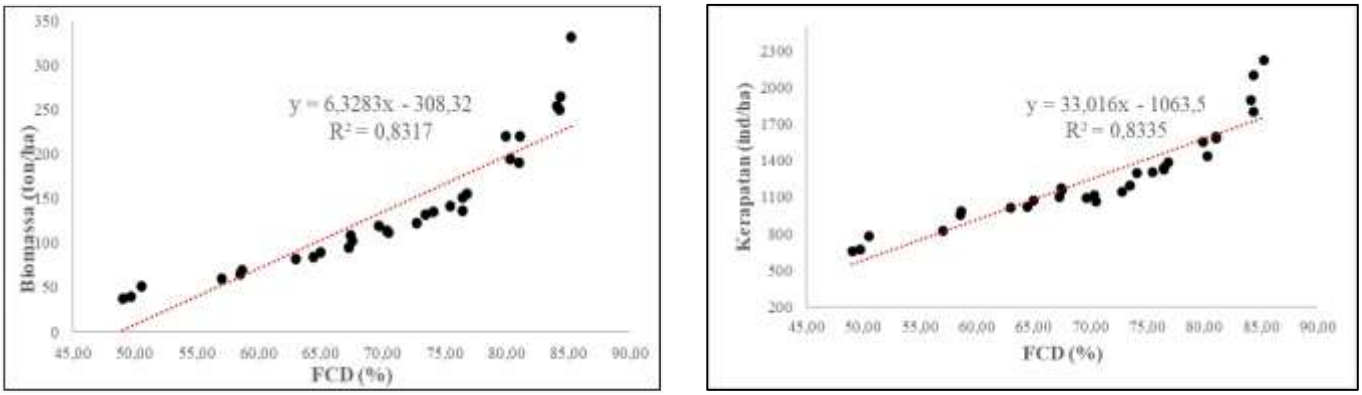

(a) (b)

Figure 7. (a) Correlation graph between FCD and biomass; (b) Correlation graph between FCD and stand density

Regression results confirm the robustness of FCD in estimating stand attributes, with $R^2 = 0.8335$ for stand density ($y = 33.016x - 1063.5$) and $R^2 = 0.8317$ for biomass ($y = 6.3283x - 308.32$). These values exceed those reported in comparable studies, particularly in heterogeneous systems, highlighting the advantage of FCD application in natural forests. Given that approximately 47–50% of biomass represents carbon (Thomas & Martin, 2012), the model provides a practical basis for spatial carbon estimation. This capability positions FCD as an efficient tool for Monitoring, Reporting, and Verification (MRV) under REDD+, enabling cost-effective assessment of carbon-related ecosystem services and supporting conservation prioritization in mining landscapes.

Conclusion

The linear regression models based on Forest Canopy Density (FCD) demonstrated strong capability in estimating both stand density and aboveground biomass. The stand density model ($*y = 33.016 \times FCD - 1063.5$; $R^2 = 0.83$; $p < 0.05*$) showed high accuracy, with an NRMSE of 12%, negligible bias (0.96 ind/ha), and very small aggregate and mean deviations (SA = 0.0008; SR = 0.00003). The biomass model ($*y = 6.3283 \times FCD - 308.32$; $R^2 = 0.83$; $p < 0.05*$) exhibited comparable performance, with an almost zero bias (−0.0002 ton/ha), although its estimation accuracy was lower (NRMSE = 22%) compared to the stand density model. Both models explain more than 83% of the variation in their respective response variables, confirming that FCD is a reliable predictor for estimating both stand density and biomass. The difference in NRMSE between the two models indicates that the allometric variability of biomass, which is not fully captured by FCD, is greater than the variability associated with stand density.

Acknowledgments

The author team would like to express their gratitude to all those involved in this research who supported this research directly or indirectly so that it could be completed and published

Author Contributions

This article was written by three authors, namely Reza D.P, Lilik B.P, and Rachmad H. All authors worked together to complete each stage of the research until it was completed.

Funding

There is no external funding.

Conflicts of Interest

The authors declare no conflict of interest in this research articles.

References

Abdollahnejad, A., Panagiotidis, D., & Surový, P. (2017). Forest canopy density assessment using different

approaches - Review. *Journal of Forest Science*, *63*(3), 107–116. https://doi.org/10.17221/110/2016-JFS

Agus, C., Pradipa, E., Wulandari, D., Supriyo, H. S., Saridi, S., & Herika, D. H. (2014). Peran Revegetasi Terhadap Restorasi Tanah Pada Lahan Rehabilitasi Tambang Batubara Di Daerah Tropika. *Jurnal Manusia Dan Lingkungan*, *21*(1), 60–66. Retrieved from http://jpe-ces.ugm.ac.id/ojs/index.php/JML/article/view/32

Aguswan, Y., Gumiri, S., Mas Sukarna, R., & Permana, I. (2022). Mapping Degraded Area for Tropical Peatland Revegetation Using Forest Canopy Density Model Landsat 8 OLI-TIRS in Central Kalimantan, Indonesia. *Environment and Natural Resources Journal*, *20*(4), 1–12. https://doi.org/10.32526/ennrj/20/202200008

Andini, W. T., Nurlina, N., & Ridwan, I. (2024). Monitoring Vegetation Change Using Forest Cover Density Model. *Ecological Engineering & Environmental Technology*, *25*(9), 369–378. https://doi.org/10.12912/27197050/190928

Arifin, Z. (2025). Carbon Sequestration Dynamics on Reclaimed Land: A Coupled Ecological-Economic Assessment in Indonesia. *Acta Fytotechnica et Zootechnica*, *28*(4), 360–369. https://doi.org/10.15414/afz.2025.28.04.360-369

Ashaari, F., Kamal, M., & Dirgahayu, D. (2018). Comparison Of Model Accuracy In Tree Canopy Density Estimation Using Single Band, Vegetation Indices And Forest Canopy Density (FCD) Based On Landsat-8 Imagery (Case Study: Peat Swamp Forest In Riau Province). *International Journal of Remote Sensing and Earth Sciences (IJReSES)*, *15*(1), 81. https://doi.org/10.30536/j.ijreses.2018.v15.a2845

Asner, G. P. (2009). Tropical forest carbon assessment: integrating satellite and airborne mapping approaches. *Environmental Research Letters*, *4*(3), 034009. https://doi.org/10.1088/1748-9326/4/3/034009

Asum, A., Adu-Bredu, S., Hayford, A., Abugre, S., Danquah, L., & Sarfo, D. A. (2024). Maximizing climate solutions: Assessing Forest plantation productivity and carbon sequestration potential of tree species. *International Journal for Multidisciplinary Research*, *6*(3). https://doi.org/10.36948/ijfmr.2024.v06i03.19593

Atmojo, A., Triyani, R., Irwansyah Fauzi, A., Ulin Nuha, M., Ramadhini, M., & Rohman, A. (2024). Model Forest Canopy Density pada Citra SPOT-6 untuk Estimasi Potensi Tegakan Pohon di Kawasan Pengelolaan Hutan Lindung Batu Serampok Lampung Selatan. *Jurnal Fisika Unand*, *13*(6), 771–783. https://doi.org/10.25077/jfu.13.6.771-783.2024

Batterman, S. A., Hedin, L. O., van Breugel, M., Ransijn, J., Craven, D. J., & Hall, J. S. (2013). Key role of symbiotic dinitrogen fixation in tropical forest secondary succession. *Nature*, *502*(7470), 224–227. https://doi.org/10.1038/nature12525

Burt, A., Calders, K., Cuni-Sanchez, A., Gómez-Dans, J., Lewis, P., Lewis, S. L., Malhi, Y., Phillips, O. L., & Disney, M. (2020). Assessment of Bias in Pan-Tropical Biomass Predictions. *Frontiers in Forests and Global Change*, *3*, 12. https://doi.org/10.3389/ffgc.2020.00012

Castellanos, P., Colarco, P., Espinosa, W. R., Guzewich, S. D., Levy, R. C., Miller, R. L., Chin, M., Kahn, R. A., Kemppinen, O., Moosmüller, H., Nowottnick, E. P., Rocha-Lima, A., Smith, M. D., Yorks, J. E., & Yu, H. (2024). Mineral dust optical properties for remote sensing and global modeling: A review. *Remote Sensing of Environment*, *303*, 113982. https://doi.org/10.1016/j.rse.2023.113982

Chave, J., Réjou-Méchain, M., Búrquez, A., Chidumayo, E., Colgan, M. S., Delitti, W. B. C., Duque, A., Eid, T., Fearnside, P. M., Goodman, R. C., Henry, M., Martínez-Yrízar, A., Mugasha, W. A., Muller-Landau, H. C., Mencuccini, M., Nelson, B. W., Ngomanda, A., Nogueira, E. M., Ortiz-Malavassi, E., … Vieilledent, G. (2014). Improved allometric models to estimate the aboveground biomass of tropical trees. *Global Change Biology*, *20*(10), 3177–3190. https://doi.org/10.1111/gcb.12629

Danoedoro, P., & Gupita, D. D. (2022). Combining Pan-Sharpening and Forest Cover Density Transformation Methods for Vegetation Mapping using Landsat-8 Satellite Imagery. *International Journal on Advanced Science, Engineering and Information Technology*, *12*(3), 881. https://doi.org/10.18517/ijaseit.12.3.12514

Dasrizal, Rahmi, Rezki, A., Farida, Ulni, A. Z. P., & Syafruddin, Y. S. (2019). Outlook for carbon stock of tropical forest in the context of climate change. *IOP Conference Series: Earth and Environmental Science*, *299*(1), 012049. https://doi.org/10.1088/1755-1315/299/1/012049

Dwiyanto, M. R., Damayanti, A., Indra, T. L., & Dimyati, M. (2021). Land Use Changes Due to Mining Activities in Penajam Paser Utara Regency, East Kalimantan Province. *Journal of Physics: Conference Series*, *1811*(1), 012088. https://doi.org/10.1088/1742-6596/1811/1/012088

Erwin, E. (1970). Short Communication: Microscopic decay pattern of yellow meranti caused by white-rot fungus Phlebia brevispora. *Biodiversitas Journal of Biological Diversity*, *17*(2), 409–416.

https://doi.org/10.13057/biodiv/d170203

Fahmi, S., Wahyudi, D., Natasya Niviani, B., Sagita Putri, A., & Al Kautsar, A. (2025). Perbandingan Pemetaan Kerapatan Kanopi Vegetasi Di Taman Hutan Raya Djuanda Menggunakan Transformasi Fcd Dan Msarvi Berdasarkan Citra Sentinel-2A. *Jurnal Hutan Tropis*, *13*(2), 303. https://doi.org/10.20527/jht.v13i2.23034

Falensky, M. A., Sulti, A. L., Putra, R. D., & Marko, K. (2020). Application of Forest Canopy Density (FCD) Model for the Hotspot Monitoring of Crown Fire in Tebo, Jambi Province. *Jurnal Geografi Lingkungan Tropik*, *4*(1). https://doi.org/10.7454/jglitrop.v4i1.76

Farosandi, N. H., Mansur, I., & Istikorini, Y. (2024). Carbon stock estimation in post-mining reclamation area of open coal mining in PT Berau Coal, Berau, East Kalimantan. *IOP Conference Series: Earth and Environmental Science*, *1315*(1), 012043. https://doi.org/10.1088/1755-1315/1315/1/012043

Fauziah, F., Fiqa, A. P., Lestari, D. A., & Budiharta, S. (2021). Carbon-stock estimation in three types of coal post-mining reclamation at East Kutai Regency, East Kalimantan. *Jurnal Penelitian Kehutanan Wallacea*, *10*(2), 189. https://doi.org/10.18330/jwallacea.2021.vol10iss2pp189-197

Foody, G. M., Cutler, M. E., McMorrow, J., Pelz, D., Tangki, H., Boyd, D. S., & Douglas, I. (2003). Mapping the biomass of Bornean tropical rain forest from remotely sensed data. *Global Ecology and Biogeography*, *12*(5), 379–387. https://doi.org/10.1046/j.1466-822X.2003.00067.x

Gao, S., Zhong, R., Yan, K., Ma, X., Chen, X., Pu, J., Gao, S., Qi, J., Yin, G., & Myneni, R. B. (2023). Evaluating the saturation effect of vegetation indices in forests using 3D radiative transfer simulations and satellite observations. *Remote Sensing of Environment*, *295*, 113665. https://doi.org/10.1016/j.rse.2023.113665

Hartoyo, A. P. P., Prasetyo, L. B., Siregar, I. Z., . S., Theilade, I., & Siregar, U. J. (2019). Carbon stock assessment using forest canopy density mapper in agroforestry land in Berau, East Kalimantan, Indonesia. *Biodiversitas Journal of Biological Diversity*, *20*(9), 2661–2676. https://doi.org/10.13057/biodiv/d200931

Hossain, M. S., Oluwajuwon, T. V., Ludgen, A. N., Hasert, D. P., Sitanggang, M., & Offiah, C. (2023). Formulating biomass allometric model for Paraserianthes falcataria (L) Nielsen (Sengon) in smallholder plantations, Central Kalimantan, Indonesia. *Forest Science and Technology*, *19*(4), 268–284. https://doi.org/10.1080/21580103.2023.2256355

Huy, B., Poudel, K., Kralicek, K., Hung, N., Khoa, P., Phương, V., & Temesgen, H. (2016). Allometric Equations for Estimating Tree Aboveground Biomass in Tropical Dipterocarp Forests of Vietnam. *Forests*, *7*(8), 180. https://doi.org/10.3390/f7080180

Isworo, S., Nuryadi, H., & Oetari, P. S. (2025). Reviving Ecosystems: Vegetation Structure and Biodiversity Recovery in Reclaimed Coal Mining Areas of Kalimantan. *Nature Environment and Pollution Technology*, *24*(4), 1–15. https://doi.org/10.46488/NEPT.2025.v24i04.D1780

Judijanto, L., & Adiwijaya, S. (2024). Dampak Eksplorasi Sumber Daya Alam Terhadap Keberlanjutan Ekosistem Hutan Tropis di Kalimantan. *Jurnal Geosains West Science*, *2*(03), 103–111. https://doi.org/10.58812/jgws.v2i03.1676

Kartikasari, R., Rachmansyah, A., & Leksono, A. S. (2019). Impact Of Coal Mining In Forest Area To Carbon Emission In Kutai Kartanegara, East Kalimantan. *Jurnal Pengelolaan Sumberdaya Alam Dan Lingkungan (Journal of Natural Resources and Environmental Management)*, *9*(4), 1066–1074. https://doi.org/10.29244/jpsl.9.4.1066-1074

Karyati, K., Karmini, K., & Widiati, K. Y. (2023). The allometric equations for estimating above-ground biomass in a 50 years-old secondary forest in East Kalimantan, Indonesia. *Biodiversitas Journal of Biological Diversity*, *24*(3), 1482–1492. https://doi.org/10.13057/biodiv/d240318

Komara, H., Sakti, A., & Harto, A. (2024). Assessing Environmental Impacts of Mining Activities in Kalimantan Using Remote Sensing Approach. *Proceedings of the 2nd International Conference on Nature-Based Solution in Climate Change, RESILIENCE 2023, 24 November 2023, Jakarta, Indonesia*, 9–18. https://doi.org/10.4108/eai.24-11-2023.2346422

Lu, D., Chen, Q., Wang, G., Liu, L., Li, G., & Moran, E. (2016). A survey of remote sensing-based aboveground biomass estimation methods in forest ecosystems. *International Journal of Digital Earth*, *9*(1), 63–105. https://doi.org/10.1080/17538947.2014.990526

Manuri, S., Brack, C., Noor'an, F., Rusolono, T., Anggraini, S. M., Dotzauer, H., & Kumara, I. (2016). Improved allometric equations for tree aboveground biomass estimation in tropical dipterocarp forests of Kalimantan, Indonesia. *Forest Ecosystems*, *3*(1), 28. https://doi.org/10.1186/s40663-016-0087-2

Marjenah, M., Matius, P., Purnomo, D. T., Kiswanto, K., & Sutedjo, S. (2023). Perubahan struktur dan

komposisi tegakan pada areal bekas tebangan sistem TPTI di Kalimantan Timur. *ULIN: Jurnal Hutan Tropis*, *7*(1), 20. https://doi.org/10.32522/ujht.v7i1.8385

Merrick, T., Pau, S., Detto, M., Broadbent, E. N., Bohlman, S., Still, C. J., & Almeyda Zambrano, A. M. (2021). Unveiling spatial and temporal heterogeneity of a tropical forest canopy using high-resolution NIRv, FCVI, and NIRvrad from UAS observations. *Biogeosciences*. https://doi.org/10.5194/bg-2021-95

Mildrexler, D. J., Zhao, M., & Running, S. W. (2011). A global comparison between station air temperatures and MODIS land surface temperatures reveals the cooling role of forests. *Journal of Geophysical Research*, *116*(G3), G03025. https://doi.org/10.1029/2010JG001486

Mutanga, O., Masenyama, A., & Sibanda, M. (2023). Spectral saturation in the remote sensing of high-density vegetation traits: A systematic review of progress, challenges, and prospects. *ISPRS Journal of Photogrammetry and Remote Sensing*, *198*, 297–309. https://doi.org/10.1016/j.isprsjprs.2023.03.010

Nellis, M. D. (2005). From the Journal Editor. *Geocarto International*, *20*(2), 3–3. https://doi.org/10.1080/10106040508542339

Nugraha, A. S. A., & Citra, I. P. A. (2021). Perbandingan Metode Soil Adjusted Vegetation Index (SAVI) dan Forest Canopy Density (FCD) untuk Identifikasi Tutupan Vegetasi (Kasus; Area Pembuatan Jalan Baru Singaraja-Mengwi). *Jurnal Geografi : Media Informasi Pengembangan Dan Profesi Kegeografian*, *18*(1), 1–8. https://doi.org/10.15294/jg.v18i1.25367

Nugraha, A. S. A., & Kurniawan, W. D. W. (2024). Thermal index effect in forest canopy density (FCD) methods based on remote sensing imagery. In C. M. Roelfsema, A. Besse Rimba, S. Arjasakusuma, & A. Blanco (Eds.), *Eighth Geoinformation Science Symposium 2023: Geoinformation Science for Sustainable Planet* (p. 9). SPIE. https://doi.org/10.1117/12.3009322

Pandey, H. P., Bhandari, S. K., & Harrison, S. (2022). Comparison among allometric models for tree biomass estimation using non-destructive trees' data. *Tropical Ecology*, *63*(2), 263–272. https://doi.org/10.1007/s42965-021-00210-0

Persson, H. J., & Ståhl, G. (2020). Characterizing Uncertainty in Forest Remote Sensing Studies. *Remote Sensing*, *12*(3), 505. https://doi.org/10.3390/rs12030505

Riefani, M. K., Soendjoto, M. A., & Munir, A. M. (2018). Short Communication: Bird species in the cement factory complex of Tarjun, South Kalimantan, Indonesia. *Biodiversitas Journal of Biological Diversity*, *20*(1), 218–225. https://doi.org/10.13057/biodiv/d200125

Rizali, A., Oktaviyani, O., Putri, S., Doananda, M., & Linggani, A. (2021). Invasion of fall armyworm Spodoptera frugiperda, a new invasive pest, alters native herbivore attack intensity and natural enemy diversity. *Biodiversitas Journal of Biological Diversity*, *22*(8), 3392–3400. https://doi.org/10.13057/biodiv/d220847

Rodríguez-Veiga, P., Quegan, S., Carreiras, J., Persson, H. J., Fransson, J. E. S., Hoscilo, A., Ziółkowski, D., Stereńczak, K., Lohberger, S., Stängel, M., Berninger, A., Siegert, F., Avitabile, V., Herold, M., Mermoz, S., Bouvet, A., Le Toan, T., Carvalhais, N., Santoro, M., … Balzter, H. (2019). Forest biomass retrieval approaches from earth observation in different biomes. *International Journal of Applied Earth Observation and Geoinformation*, *77*, 53–68. https://doi.org/10.1016/j.jag.2018.12.008

Rosikin, R., Prasetyo, L. B., & Hermawan, R. (2023). Assessment of the success of canopy cover revegetation of former coal mine lands with Forest Canopy Density (FCD) Model in Kutai Kartanegara, East Kalimantan. *Jurnal Pengelolaan Sumberdaya Alam Dan Lingkungan (Journal of Natural Resources and Environmental Management)*, *13*(4), 574–585. https://doi.org/10.29244/jpsl.13.4.574-585

Saleh, M. B., Daerangga, M., Prasetyo, L. B., Setiawan, Y., Hudjimartsu, S. A., & Wijayanto, A. K. (2024). Canopy Density Estimation Model in Peat Swamp Forest Using LiDAR Data and Landsat 8 OLI Satellite Imagery. *Media Konservasi*, *29*(2), 249–262. https://doi.org/10.29244/medkon.29.2.249

Siqueira-Gay, J., Sonter, L. J., & Sánchez, L. E. (2020). Exploring potential impacts of mining on forest loss and fragmentation within a biodiverse region of Brazil's northeastern Amazon. *Resources Policy*, *67*, 101662. https://doi.org/10.1016/j.resourpol.2020.101662

Sukarna, R. M., Birawa, C., & Junaedi, A. (2021). Mapping Above-Ground Carbon Stock of Secondary Peat Swamp Forest Using Forest Canopy Density Model Landsat 8 OLI-TIRS: A Case Study in Central Kalimantan Indonesia. *Environment and Natural Resources Journal*, *19*(2), 165–175. https://doi.org/10.32526/ennrj/19/2020209

Thomas, S. C., & Martin, A. R. (2012). Carbon Content of Tree Tissues: A Synthesis. *Forests*, *3*(2), 332–352. https://doi.org/10.3390/f3020332

Tian, J., Dong, P., Xing, Y., Shan, W., Wang, Q., & Li, D. (2023). Comparison between biophysical analysis model and dimidiate pixel model for the estimation of forest canopy density. *Journal of*

Applied Remote Sensing, *17*(01), 14518. https://doi.org/10.1117/1.JRS.17.014518

Wang, H., Muller, J. D., Tatarinov, F., Yakir, D., & Rotenberg, E. (2022). Disentangling Soil, Shade, and Tree Canopy Contributions to Mixed Satellite Vegetation Indices in a Sparse Dry Forest. *Remote Sensing*, *14*(15), 3681. https://doi.org/10.3390/rs14153681

Werdana, K. P., Megantara, E. N., Withaningsih, S., & Saputra, Y. H. E. (2024). Allometric equation of Paraserianthes falcataria (L.) and Anthocephalus cadamba Miq. for estimating carbon stocks. *Jurnal Presipitasi : Media Komunikasi Dan Pengembangan Teknik Lingkungan*, *21*(2), 609–621. https://doi.org/10.14710/presipitasi.v21i2.609-621

Williams, B. A., Grantham, H. S., Watson, J. E. M., Shapiro, A. C., Plumptre, A. J., Ayebare, S., Goldman, E., & Tulloch, A. I. T. (2022). Reconsidering priorities for forest conservation when considering the threats of mining and armed conflict. *Ambio*, *51*(9), 2007–2024. https://doi.org/10.1007/s13280-022-01724-0

Yunanto, T., Mitlöhner, R., & Bürger-Arndt, R. (2019). Vegetation development and the condition of natural regeneration after coal mine reclamation in East Kalimantan, Indonesia. *Proceedings of the International Conference on Mine Closure*, *2019-September*, 1289–1302. https://doi.org/10.36487/ACG_rep/1915_102_Yunanto

Zhao, P., Lu, D., Wang, G., Wu, C., Huang, Y., & Yu, S. (2016). Examining Spectral Reflectance Saturation in Landsat Imagery and Corresponding Solutions to Improve Forest Aboveground Biomass Estimation. *Remote Sensing*, *8*(6), 469. https://doi.org/10.3390/rs8060469